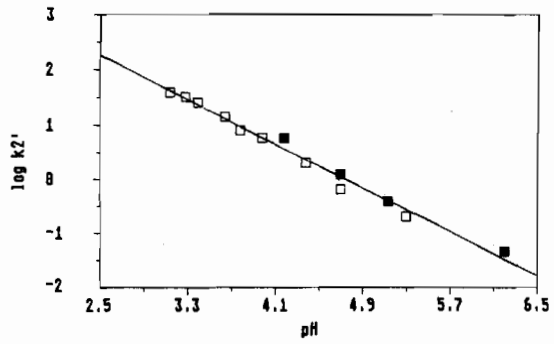

Figure 8. Comparison of the k_2' data obtained for Fe(edta) (□) and NO_2^- (■) in excess where $k_2' = k_{obsd}/[Fe^{II}(edta)] = k_2[H^+]/([H^+] + K_a)$ (see eq 4) or $k_2' = k_B/2[\text{total } NO_2^-] = k_2[H^+]/([H^+] + K_a)$ (see eq 9).

as NO^+ on the basis of recent reports in the literature,[14,19] but it might be N_2O_3, which will react in a similar manner in the subsequent non-rate-determining steps. It is encouraging to note that the values of k_2, obtained in two completely different ways, are so similar. A comparison of these data as a function of pH is presented in Figure 8. The data for the process with excess Fe^{II}(edta) is expressed as $k_{obsd}/[Fe^{II}(edta)]$ and for the reaction with excess nitrite as $k_B/2[\text{total } NO_2^-]$ according to eq 4 and 9, respectively. The pH dependence of these data arises solely from the fraction of nitrite present as HONO, which decreases with increasing pH.

A comparison of our results for the Fe^{II}(edta)/HONO/NO_2^- system with those reported in the literature reveals that although the studies were carried out under different conditions, the results correlate well. Uchiyama et al.[18] followed the formation of Fe^{II}(edta)NO using a method referred to as concentration-step controlled-potential electrolysis. They worked with an excess of Fe^{II}(edta) and therefore only observed the pseudo-first-order reaction path. We have extrapolated a second-order rate constant (k_2) of 50 M^{-1} s^{-1} from their data, which is very close to that reported in this study. Shearer[11] studied the system in detail but used a different procedure for the calculation of the rate constants. The second-order rate constants extrapolated from his data with use of plots of log k_{obsd} vs log [HONO] are $k_4 = 11$ M^{-1} s^{-1} and $k_2 = 41$ M^{-1} s^{-1}, once again in fair agreement with our findings. His suggested mechanism is very similar to ours except for his choice of NO_2^- as the reactive species. It is also important to note that he was unable to detect the square dependence of the pseudo-zero-order rate constant on [HONO] from his limited pH-dependence study.

The results of this study clearly demonstrate how the formation of Fe^{II}(edta)NO can occur along different reaction routes depending on the experimental conditions employed. In the absence of oxygen, Fe^{II}(edta) will pick up NO on a microsecond time scale. In the presence of oxygen, NO will be partially oxidized to HONO/NO_2^- (as evidenced by the characteristic fingerprint spectrum observed for HONO at low pH in the range 300–400 nm[24]) and Fe^{II}(edta) to Fe^{III}(edta). Under such conditions, HONO is the reactive species and is responsible either for the formation of NO^+ (or N_2O_3) or for the formation of NO via the oxidation of Fe^{II}(edta) to Fe^{III}(edta). It follows that the complete process is controlled by [O_2], pH, and [total NO_2^-] since these factors control the balance between the various reaction routes.

The rapid formation of Fe^{II}(edta)NO is most probably due to the presence of a labile water molecule in the coordination sphere of Fe^{II}(edta). Although we have no direct evidence for the presence of such a water molecule, the observed reactivity, as well as studies on the closely related Ru^{III}(edta) system,[25-27] suggest this to be the case. A ring-opened edta ligand can via hydrogen bonding labilize the coordinated water molecule or enable an associative attack of the entering ligand. Protonation of such a species (at pH <3 in our case) will decrease this interaction and account for the decrease in reactivity observed under such conditions. In this respect it is important to note that recent Mössbauer spectroscopic studies of the Fe^{II}(edta) system[28] suggest the formation of a protonated species at pH 2.5. It is therefore quite realistic to formulate the complex as Fe^{II}(edta)H_2O, in which the edta ligand occupies five coordination sites and the ring-opened edta ligand is protonated at pH <3.

Acknowledgment. We gratefully acknowledge financial support from the Deutsche Forschungsgesellschaft, the Fonds der Chemischen Industrie, and the Max-Buchner Forschungsstiftung.

Registry No. Fe^{II}(edta), 21393-59-9; HONO, 7782-77-6; NO_2^-, 14797-65-0.

(24) Stockwell, W. R.; Calvert, J. G. *J. Photochem.* **1978**, *8*, 193.
(25) Matsubara, T.; Creutz, C. *J. Am. Chem. Soc.* **1978**, *100*, 6255.
(26) Matsubara, T.; Creutz, C. *Inorg. Chem.* **1979**, *18*, 1956.
(27) Bajaj, H. C.; van Eldik, R. *Inorg. Chem.*, in press.
(28) Marton, A.; Sükösd-Rozlosnik, N.; Vértes, A.; Nagy-Czakó, I.; Burger, K. *Inorg. Chim. Acta* **1987**, *137*, 173.

Contribution from the Department of Chemistry,
The University of North Carolina at Chapel Hill, Chapel Hill, North Carolina 27514

Redox Properties and Ligand Loss Chemistry in Aqua/Hydroxo/Oxo Complexes Derived from *cis*- and *trans*-$[(bpy)_2Ru^{II}(OH_2)_2]^{2+}$

John C. Dobson and Thomas J. Meyer*

Received December 14, 1987

Electrochemical studies on the cis and trans isomers of $[(bpy)_2Ru^{II}(OH_2)_2]^{2+}$ (bpy is 2,2′-bipyridine) as a function of pH in aqueous solution have revealed the existence of a series of pH-dependent redox couples that interconvert oxidation states II → VI. The electrochemical data give insight into the relative stabilities of the cis and trans isomers as well the stabilities of individual oxidation states. In acidic solution, oxidation state VI for the cis complex is unstable with respect to ligand loss and the resulting Ru(VI) complex is unstable with respect to reduction to Ru(III). Comparisons with redox potentials for related couples allow a qualitative assessment to be made concerning the role of electronic structure in determining the magnitudes of redox potentials and of the possible use of monomeric aqua/hydroxo/oxo couples as four-electron oxidants for the catalytic oxidation of water to molecular oxygen.

Introduction

The oxidation of water to molecular oxygen is a problem of both technological and fundamental interest. One of our concerns has been with the design of molecular catalysts for water oxidation that could conceivably be integrated into more complex photochemical or electrochemical energy conversion systems.[1] We and others have shown that the μ-oxo ion $[(bpy)_2(OH_2)RuORu(OH_2)(bpy)_2]^{4+}$ (bpy is 2,2′-bipyridine) and its derivatives are

(1) See, for example: (a) *Energy Resources through Photochemistry and Catalysis*; Gratzel, M., Ed.; Academic: New York, 1983. (b) *Chemically Modified Surfaces in Catalysis and Electrocatalysis*; Miller, J. S., Ed.; American Chemical Society: Washington, DC, 1982.

0020-1669/88/1327-3283$01.50/0

catalysts for the oxidation of water.[2] In earlier work it was shown that the oxidation of *cis*-$[(bpy)_2Ru^{II}(H_2O)_2]^{2+}$ to *cis*-$[(bpy)_2Ru^{VI}(O)_2]^{2+}$ occurs by a series of electron–proton loss steps and, from redox potential measurements, that the complex *cis*-$[(bpy)_2Ru^{VI}(O)_2]^{2+}$ is, in principle, capable of the oxidation of water to dioxygen via the Ru(VI)/Ru(II) couple, for which $E^{\circ\prime}$ = 1.26 V vs NHE at pH 0.[3]

$$cis\text{-}[(bpy)_2Ru^{VI}(O)_2]^{2+} + 4e^- + 4H^+ \rightarrow cis\text{-}[(bpy)_2Ru^{II}(OH_2)_2]^{2+}$$

In fact, it has been reported that the higher oxidation states of $[(bpy)_2Ru(OH_2)_2]^{2+}$ in hectorite clays catalyze the oxidation of water to dioxygen,[4] although in a recent study in solution it was concluded that the complex shows little, if any, intrinsic catalytic activity toward the oxidation of water to molecular oxygen.[2b]

We report here the results of a study on the redox and stability properties of the monomeric diaqua complexes *cis*- and *trans*-$[(bpy)_2Ru(OH_2)_2]^{2+}$. Our interests in the complexes were severalfold: (1) We wanted to explore the possible role of monomeric complexes as catalytic or stoichiometric reagents for the oxidation of water. (2) We wished to make comparisons with the properties of related complexes of Os. (3) We hoped to gain sufficient insight into the underlying redox and coordination chemistry to explore the possible development of metal–oxo-based oxidation catalysts. (4) We wished to extend the initial observations made by Takeuchi et al.[3] and Che et al.[5] on these systems and to contribute to the expanding chemistry of the oxo complexes of Ru and Os.[6]

Experimental Section

Materials. Ceric ammonium nitrate, $(NH_4)_2Ce(NO_3)_6$, was purchased from Fisher Scientific Co. and dried in vacuo prior to use. Buffer solutions for electrochemical measurements were prepared from aqueous $HClO_4$ with $LiClO_4$ added as additional electrolyte (pH 0–2) and mono-, di-, and tribasic phosphate solutions (pH >2) to maintain a minimum ionic strength of 0.1 M. The pH measurements were made after addition of the complex to the buffer solution by using a radiometer pHM62 pH meter. Trifluoromethanesulfonic acid was purchased from Aldrich Chemical Co. The ligand 4,4′-dimethyl-2,2′-bipyridine (Reilly Tar and Chemical Co.) was recrystallized from acetone. The ligand 5,5′-dimethyl-2,2′-bipyridine was a gift from Dr. Joseph Conner. All other materials were obtained as reagent grade and used without further purification.

Preparations. A procedure for the preparation of *cis*-$[(bpy)_2Ru(CO_3)]\cdot 2H_2O$ has been reported previously.[7a]

***trans*-$[(bpy)_2Ru^{II}(OH_2)_2](CF_3SO_3)_2$.** The procedure described here is a modification of one that has appeared previously.[7b] To 15 mL of 0.1 M CF_3SO_3H (aqueous) was added 50 mg (0.098 mmol) of *cis*-$[(bpy)_2Ru(CO_3)]\cdot 2H_2O$. The solution was stirred for 20 min and allowed to stand in room light for 24 h after which time isomerization led to the formation of black crystals of the desired complex. The solid was collected on a medium glass frit and washed with 5 mL of cold distilled water. If aqueous $HClO_4$ is used rather than aqueous CF_3SO_3H complications appear from oxidation to the oxidized analogue *trans*-$[(bpy)_2Ru^{III}(OH)(OH_2)]^{2+}$. Yield: 66 mg, 90%. Anal. Calcd for $RuC_{22}H_{20}N_4O_8F_6S_2$: C, 35.33; H, 2.68; N, 7.49. Found: C, 35.49; H, 2.70; N, 7.45.

***cis*-$[(5,5'\text{-dmbp})_2RuCl_2]\cdot H_2O$ and *cis*-$[(4,4'\text{-dmbp})_2RuCl_2]\cdot 2H_2O$.** The two bpy-substituted complexes were prepared in a manner similar to that reported previously for *cis*-$[(bpy)_2RuCl_2]\cdot 2H_2O$ but using either 5,5′-dimethyl-2,2′-bipyridine (5,5′-dmbp) or 4,4′-dimethyl-2,2′-bipyridine (4,4′-dmbp) in place of bpy.[8]

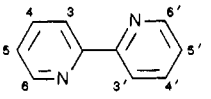

bpy

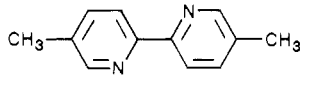

5,5′-dmbp

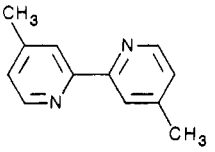

4,4′-dmbp

Small amounts of the CO-containing complexes *cis*-$[(bpy)_2Ru^{II}(CO)(Cl)]^+$[2b,9] also appear as products, but washing with 5 × 15-mL portions of cold distilled H_2O removes both excess LiCl and the CO-containing complex from the isolated solid. The purity of the products was established by cyclic voltammetry ($E_{1/2}Ru^{III/II}$ = 0.25 V vs SSCE, CH_3CN/0.1 M tetra-*n*-butylammonium hexafluorophosphate for the 5,5′-dmbp complex and 0.19 V for the 4,4′-dmbp complex) and elemental analysis. Anal. Calcd for $RuC_{24}H_{24}N_4Cl_2$ (*cis*-$[(5,5'\text{-dmbp})_2RuCl_2]\cdot H_2O$): C, 51.61; H, 4.66; N, 10.03; Cl, 12.72. Found: C, 51.02; H, 4.88; N, 9.88; Cl, 12.39.

***cis*-$[(5,5'\text{-dmbp})_2Ru(CO_3)]\cdot 3H_2O$.** To 40 mL of argon-degassed house-distilled H_2O was added 1.0 g of *cis*-$[(5,5'\text{-dmbp})_2RuCl_2]\cdot H_2O$ and 3.0 g of Na_2CO_3. The solution was heated at reflux under argon for 1 h, allowed to cool to room temperature, and placed in a refrigerator for 15 min. The solution was filtered onto a medium glass frit, washed with 5 × 1 mL portions of cold 10^{-3} M aqueous NaOH and dried in vacuo. Yield: 0.95 g, 88%. Anal. Calcd for $RuC_{25}H_{30}O_6N_4$: C, 51.45; H, 5.14; N, 9.60. Found: C, 50.67; H, 4.99; N, 9.75.

***cis*-$[(4,4'\text{-dmpb})_2Ru(CO_3)]\cdot 5H_2O$.** The same procedure as described above for *cis*-$[(5,5'\text{-dmbp})_2Ru(CO_3)]\cdot 3H_2O$ was followed but using *cis*-$[(4,4'\text{-dmbp})_2RuCl_2]\cdot 3H_2O$ as the starting material. Yield: 85%. Anal. Calcd for $RuC_{25}H_{34}O_8N_4$: C, 48.46; H, 5.49; N, 9.0. Found: C, 48.05; H, 5.12; N, 8.96.

Aqueous solutions of *cis*-$[(bpy)_2Ru^{II}(OH_2)_2]^{2+}$ were prepared by dissolving the appropriate amount of *cis*-$[(bpy)_2Ru(CO_3)]\cdot 2H_2O$ in acidic solutions. The diaqua complex is formed by protonation and loss of carbonate as CO_2.

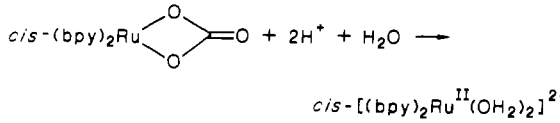

Measurements. Routine UV–vis spectra were recorded in quartz cells at room temperature on a Hewlett-Packard Model 8450A diode array spectrometer. Spectroelectrochemical experiments were carried out under argon by using an all-quartz three-compartment cell with quartz frits. Proton NMR spectra were recorded in D_2O on a Varian VXR 400 MHz FT-NMR and referenced to sodium 2,2-dimethyl-silapentane-5-sulfonate (DSS).

Electrochemical measurements were made by using a PAR Model 173 potentiostat with a PAR Model 175 universal programmer as a sweep generator of voltammetric experiments. Measurements were made vs the saturated sodium chloride calomel electrode (SSCE) at 25 ± 2 °C and are uncorrected for junction potential effects. Cyclic voltammetric experiments were performed on argon-degassed solutions in a three-compartment cell using a ~0.07 cm^2 glassy-carbon disk electrode (Tokai Carbon, Inc., Japan) as the working electrode and a platinum wire as the auxiliary electrode. The reversibility of the higher oxidation state redox couples is sensitive to the electrode surface. Reproducible results were obtained by polishing the glassy-carbon disk electrode with 1 μm alumina just prior to use. Coulometry experiments were performed in three-component cells using coarse (12 holes per linear inch) reticulated vitreous carbon (ERG, Inc.) connected to a copper wire with conductive carbon paint (SPI Supplies). Electrolysis experiments were continued

(2) (a) Gilbert, J. A.; Eggleston, D. S.; Murphy, W. R., Jr.; Geselowitz, D. A.; Gersten, S. W.; Hodgson, D. J.; Meyer, T. J. *J. Am. Chem. Soc.* **1985**, *107*, 3855. (b) Collin, J. P.; Sauvage, J. P. *Inorg. Chem.* **1986**, *22*, 1407. (c) Gersten, S. W.; Samuels, G. J.; Meyer, T. J. *J. Am. Chem. Soc.* **1982**, *104*, 4029. (d) Honda, K.; Frank, A. J. *J. Chem. Soc., Chem. Commun.* **1984**, 1635.
(3) Takeuchi, K. J.; Samuels, G. J.; Gersten, S. W.; Gilbert, J. A.; Meyer, T. J. *Inorg. Chem.* **1983**, *22*, 1407.
(4) Nijs, H.; Cruz, M. I.; Fripiat, J. J.; Van Dame, H. *Nouv. J. Chim.* **1982**, *6*, 551.
(5) Che, C. M.; Wong, K. Y.; Leung, W. H.; Poon, C. K. *Inorg. Chem.* **1986**, *25*, 345.
(6) (a) Che, C. M.; Leung, W. H.; Poon, C. K. *J. Chem. Soc., Chem. Commun.* **1987**, 173. (b) Green, G.; Griffith, W. P.; Hollingshead, D. M.; Ley, S. V.; Schroeder, M. *J. Chem. Soc., Perkins Trans. 1* **1984**, 681. (c) Bailey, C. L.; Drago, R. S. *J. Chem. Soc., Chem. Commun.* **1987**, 179. (d) Goswami, S.; Chakravarty, A. R.; Chakravarty, A. *J. Chem. Soc., Chem. Commun.* **1982**, 1288.
(7) (a) Johnson, E. C.; Sullivan, B. P.; Salmon, D. J.; Adeyemi, S. A.; Meyer, T. J. *Inorg. Chem.* **1978**, *17*, 2211. (b) Durham, B.; Wilson, S. R.; Hodgson, D. J.; Meyer, T. J. *J. Am. Chem. Soc.* **1980**, *102*, 600. (c) Moyer, B. A. Ph.D. Dissertation, University of North Carolina, Chapel Hill, NC, 1979. (d) Walsh, J. L.; Durham, B. *Inorg. Chem.* **1982**, *21*, 329.
(8) Sullivan, B. P.; Salmon, D. J.; Meyer, T. J. *Inorg. Chem.* **1978**, *17*, 3334.
(9) Choudhury, D.; Jones, R. F.; Smith, G.; Cole-Hamilton, D. J. *J. Chem. Soc., Dalton Trans.* **1982**, 1143.

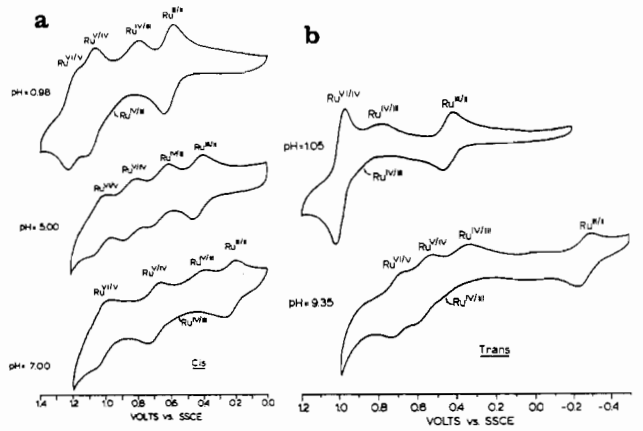

Figure 1. Representative cyclic voltammograms vs SSCE of solutions containing (a) ~2 mM *cis*-$[(bpy)_2Ru^{II}(OH_2)]^{2+}$ at various pH values (glassy-carbon working electrode, 100 mV/s, μ = 0.1 M) and (b) ~1 mM *trans*-$[(bpy)_2Ru^{II}(OH_2)_2]^{2+}$ obtained at pH values of 1.05 and 9.35 (50 mV/s, μ = 0.1 M).

until the current level reached that of the background, which was typically <5% of the initial current.

Measurements of dioxygen in the gas phase were carried out by using a Hewlett-Packard Model 5890 gas chromatograph equipped with a 5-Å molecular sieve column (Alltech Assoc.). The column temperature was 30 °C, and the helium carrier gas flow rate was 30 mL/min. A peak height vs microliter injected calibration curve was constructed from a series of injections of atmospheric air. Fifty microliter samples were syringed from the two-compartment airtight cell, and the quantities of O_2 produced were then extrapolated by using the known volume (5 mL) above the solution in the cell. No attempt was made to correct for the relatively small amount of O_2 dissolved in solution.

Results

Redox Properties. The results of cyclic voltammetric experiments on aqueous solutions containing *cis*-$[(bpy)_2Ru^{II}(OH_2)_2]^{2+}$ (Figure 1a) show that oxidation states II → VI are accessible over the narrow potential range of ~0.6 V. At pH 0.98 in 0.1 M aqueous CF_3SO_3H, a reversible wave appears at $E_{1/2}$ = 0.65 V (ΔE_p = 60 mV at 100 mV/s) for the expected Ru(III)/Ru(II) couple. In addition, a kinetically slow Ru(IV)/Ru(III) couple appears as an oxidative shoulder at $E_{p,a}$ ~ 1.02 V with $E_{p,c}$ = 0.75 V, and reversible waves for the Ru(V)/Ru(IV) and Ru(VI)/Ru(V) couples appear at $E_{1/2}$ = 1.10 and 1.26 V, respectively. At certain pH values it is possible to obtain ΔE_p values of less than 100 mV for the Ru(IV)/Ru(III) couple by using an "activated" electrode.[10] For consistency, however, an unactivated glassy-carbon electrode was used throughout the pH-dependent studies. The various redox couples are pH-dependent, and additional cyclic voltammograms taken at pH 5 and 7 again show that oxidation states II → VI are accessible over a narrow potential range.

The slowness of the Ru(IV)/Ru(III) couple appears to be associated, at least in part, with the thermodynamic consequences of the loss of protons and formation of the metal–oxo group. Either initial oxidation, $Ru^{III}—OH^{2+} \rightarrow Ru^{IV}=O^{2+}$, followed by proton loss, or initial proton loss, $Ru^{III}—OH^{2+} \rightarrow Ru^{III}—O^{+} + H^{+}$, followed by electron transfer, involve high-energy intermediates with regard to proton content as in $Ru^{IV}=OH^{3+}$ or $Ru^{III}—O^{+}$ and an additional contribution to the barrier to electron transfer at the electrode. For the related Ru(IV)/Ru(III) and Ru(III)/Ru(II) couples, *cis*-$[(bpy)_2(py)Ru^{IV}(O)]^{2+}$/$[(bpy)_2(py)Ru^{III}(OH)]^{2+}$ and *cis*-$[(bpy)_2(py)Ru^{III}(OH)]^{2+}$/$[(bpy)_2(py)Ru^{II}(OH_2)]^{2+}$, evidence is available[11] to suggest that the direct electrode reaction for the Ru(IV)/Ru(III) couple is slow and that the actual mechanism involves initial disproportionation of Ru(III)

$$2[(bpy)_2(py)Ru^{III}(OH)]^{2+} \rightarrow [(bpy)_2(py)Ru^{IV}(O)]^{2+} + [(bpy)_2(py)Ru^{II}(OH_2)]^{2+}$$

which is disfavored by ~100 mV from pH 1 to 10. For the analogous Ru(IV)/Ru(III) and Ru(III)/Ru(II) diaqua-based couples the difference in potential between the Ru(IV)/Ru(III) and Ru(III)/Ru(II) couples is ≥240 mV from pH 1 to 7, which apparently imposes a large barrier to disproportionation and removes it as a facile alternative to the direct reaction at the electrode. If the Ru(IV) → Ru(V) oxidation is more rapid, another contribution to the current–potential profile for the Ru(IV)/Ru(III) couple exists based on comproportionation between Ru(III) and Ru(V) once Ru(V) appears at the electrode (Scheme I). Given the slowness of the Ru(IV)/Ru(III) couple, the appearance of the more nearly reversible Ru(V)/Ru(IV) and Ru(VI)/Ru(V) couples (Figure 1) probably relies on the existence of the comproportionation pathway. In a separate experiment, solutions 2.19 × 10^{-4} M in *cis*-$[(bpy)_2Ru^{III}(OH_2)]^{3+}$ and *cis*-$[(bpy)_2Ru^{V}(O)(OH)]^{2+}$ in 0.1 M aqueous CF_3SO_3H were generated from the same stock solution of *cis*-$[(bpy)_2Ru^{II}(OH_2)_2]^{2+}$ by controlled-potential electrolysis at 0.75 V vs SSCE and 1.15 V vs SSCE, respectively. A second-order rate constant of 4.8 × 10^4 ± 10% M^{-1} s^{-1} for the comproportionation reaction at 22 ± 2 °C was obtained based on stopped-flow kinetic measurements and an analysis based on equivalent concentration second-order kinetics.

Scheme I. Cis Complex, pH 1

$$[(bpy)_2Ru^{II}(OH_2)_2]^{2+} \underset{+e^-}{\overset{-e^-}{\rightleftharpoons}} [(bpy)_2Ru^{III}(OH_2)_2]^{3+}$$

$$[(bpy)_2Ru^{III}(OH_2)_2]^{3+} \underset{+e^-,\,+H^+}{\overset{-e^-,\,-H^+}{\rightleftharpoons}} [(bpy)_2Ru^{IV}(O)(OH_2)]^{3+} \text{ (slow)}$$

$$[(bpy)_2Ru^{IV}(O)(OH_2)]^{3+} \underset{+e^-,\,+H^+}{\overset{-e^-,\,-H^+}{\rightleftharpoons}} [(bpy)_2Ru^{V}(O)(OH)]^{2+}$$

$$[(bpy)_2Ru^{V}(O)(OH)]^{2+} + [(bpy)_2Ru^{III}(OH)(OH_2)]^{2+} \underset{}{\overset{k = 4 \times 10^4\ M^{-1}\ s^{-1}}{\rightleftharpoons}} 2[(bpy)_2Ru^{IV}(O)(OH_2)]^{2+} \text{ (comproportionation)}$$

Kinetic effects play a far less important role for the Ru(III)/Ru(II), Ru(V)/Ru(IV), and Ru(VI)/Ru(V) couples, and an important factor, no doubt, is the easier accessibility in a thermodynamic sense of intermediates of lower proton content such as $[(bpy)_2(py)Ru^{III}(OH)]^{2+}$ or $[(bpy)_2(py)Ru^{II}(OH)]^{+}$. At 25 °C, μ = 1.0 M, pK_a values for $[(bpy)_2(py)Ru^{III}(OH_2)]^{3+}$ and $[(bpy)_2(py)Ru^{II}(OH_2)]^{2+}$ are 0.85 and 10.79, respectively.[11,12]

Controlled-potential electrolysis experiments confirm the presence of four one-electron redox processes at pH 1 for the cis complex. Electrolysis of a solution containing *cis*-$[(bpy)_2Ru^{II}(OH_2)_2]^{2+}$ in 0.1 M aqueous CF_3SO_3H at 0.75 V vs SSCE occurs with n = 0.9 ± 0.1. Further electrolysis at 1.15 V occurs with n = 1.9 ± 0.2, consistent with two-electron oxidation from Ru(III) to Ru(IV) and Ru(IV) to Ru(V). Finally, subsequent electrolysis at 1.35 V occurs with n = 1.0 ± 0.2, which is consistent with the further one-electron oxidation of Ru(V) to Ru(VI). In a separate experiment the UV–vis spectral changes associated with the four separate redox processes were monitored spectroelectrochemically, and the results are shown in Figure 2a. The spectra in the figure show that oxidation of Ru(II) to Ru(III) leads to loss of the metal to ligand charge-transfer band [$d\pi(Ru^{II}) \rightarrow \pi^*(bpy)$] at 480 nm and the appearance of a characteristic, broad ligand to metal charge-transfer band at ~355 nm for Ru(III).[13] The absorption spectra of the Ru(IV) and Ru(V) complexes are relatively featureless and show a broad band tailing to low energy that arises from bpy-localized $\pi \rightarrow \pi^*$ transitions in the UV region.

The various redox couples observed by cyclic voltammetry for *cis*-$[(bpy)_2Ru^{II}(OH_2)_2]^{2+}$ are pH-dependent, and the dependences

(10) Cabaniss, G. E.; Diamantis, A. A.; Murphy, W. R., Jr.; Linton, R. W.; Meyer, T. J. *J. Am. Chem. Soc.* **1985**, *107*, 1846.
(11) Binstead, R. A.; Meyer, T. J. *J. Am. Chem. Soc.* **1987**, *109*, 3287.
(12) (a) Moyer, B. A.; Meyer, T. J. *J. Am. Chem. Soc.* **1978**, *100*, 3601. (b) Moyer, B. A.; Meyer, T. J. *Inorg. Chem.* **1981**, *20*, 436.
(13) (a) Bryant, G. M.; Ferguson, T. E.; Powell, H. K. *Aust. J. Chem.* **1971**, *24*, 257. (b) Balzani, V.; Bolletta, F.; Gandolf, M. T.; Maestri, M. *Top. Curr. Chem.* **1978**, *75*, 1.

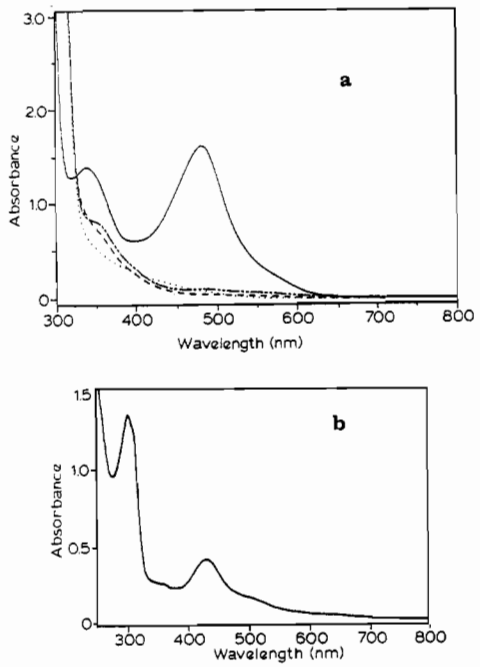

Figure 2. (a) UV–vis spectra that appear following the electrochemical oxidation of a solution of ~2.1 × 10^{-4} M *cis*-$[(bpy)_2Ru^{II}(OH_2)_2]^{2+}$ in 0.1 M aqueous CF_3SO_3H. Spectra were recorded before electrolysis (—), following electrolysis at 0.75 V vs SSCE to generate Ru(III) (—--), following electrolysis at 0.98 V vs. SSCE to generate Ru(IV) (--), and following electrolysis at 1.12 V vs SSCE to generate Ru(V) (···). (b) UV–vis spectrum obtained following decomposition of *cis*-$[(bpy)_2Ru^{VI}(O)_2]^{2+}$. The spectrum was recorded in 0.1 M aqueous CF_3SO_3H at t = ~60 min following the addition of 4 equiv of Ce(IV) to a solution of *cis*-$[(bpy)_2Ru^{II}(OH_2)_2]^{2+}$ (1 × 10^{-4} M).

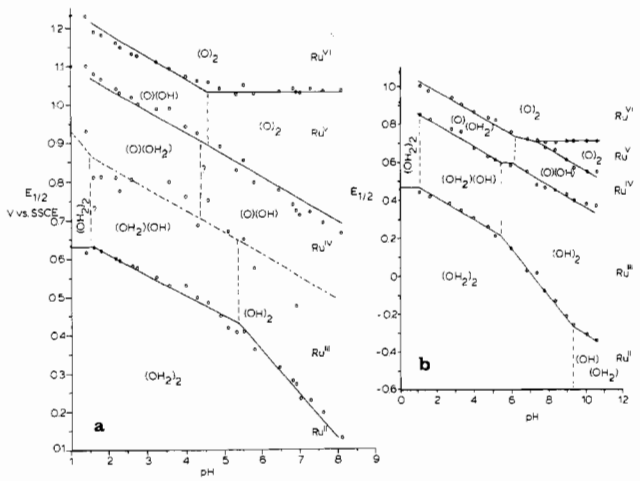

Figure 3. $E_{1/2}$ vs pH diagram for (a) *cis*-$[(bpy)_2Ru^{II}(OH_2)_2]^{2+}$ and (b) *trans*-$[(bpy)_2Ru^{II}(OH_2)_2]^{2+}$. The pH–potential regions of stability for the various oxidation states of the complex are labeled as Ru^{II}, Ru^{III}, etc. The proton compositions of the various oxidation state forms are indicated, for example, by $(OH_2)_2$–Ru^{II} for *cis*-$[(bpy)_2Ru^{II}(OH_2)_2]^{2+}$. The lines through the experimental points represent $E_{1/2}$ values for the couple indicated. Vertical lines are drawn from the breaks in the $E_{1/2}$ lines and represent approximate pK_a values. The scatter in the points for the cis Ru(IV)/Ru(III) couple is a consequence of the electrochemical irreversibility of the couple and the resulting difficulty in estimating $E_{1/2}$ values.

of the potentials as a function of pH are shown in the $E_{1/2}$–pH diagram in Figure 3a. In the diagram the oxidation state at the metal and its aqua/hydroxo/oxo compositions are indicated by abbreviations like $Ru^{III}(OH)(OH_2)$ for $[(bpy)_2Ru^{III}(OH)(OH_2)]^{2+}$. The lines show how the potentials of the couples vary with pH. Data points on the diagram are $E_{1/2}$ values obtained by cyclic voltammetry. The lines were drawn according to the Nernst equation with slopes of 0, −30, or −59 mV/pH unit corresponding to proton to electron ratios of 0, 0.5, and 1.0. Because of the large experimental uncertainty in assigning an $E_{1/2}$ value for the electrochemically irreversible Ru(IV)/Ru(III) couple (ΔE_p > 150 mV), a dashed line is used to suggest the $E_{1/2}$–pH profile. We estimate the maximum uncertainty in the individual points to be ±5%. The suggested pH dependence for the Ru(IV)/Ru(III) couple is demanded by the pH dependences of the adjacent Ru(V)/Ru(IV) and Ru(III)/Ru(II) couples for which the pH dependences are well established by the electrochemical data.

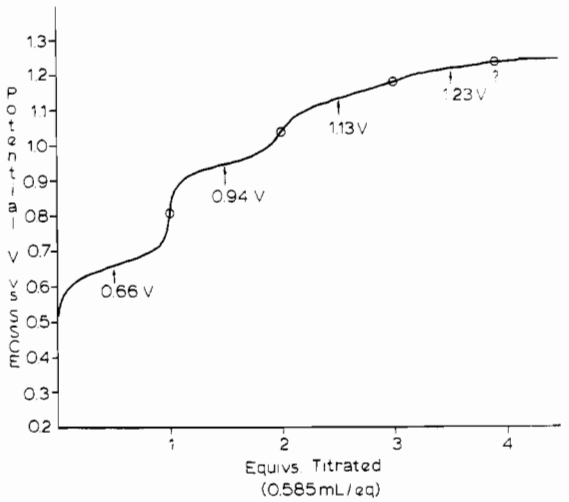

Figure 4. Potentiometric titration (vs SSCE) of 2.91 mg of *cis*-$[(bpy)_2RuCO_3]\cdot 2H_2O$ dissolved in ~5 mL of 0.1 M aqueous CF_3SO_3H by using 0.01 M $(NH_4)_2Ce(NO_3)_6$ in 0.1 M aqueous CF_3SO_3H as titrant.

Table I. $E_{1/2}$ Values Obtained by Cyclic Voltammetry for Redox Couples Associated with Diaqua Complexes of Ru(II) in 0.1 M Aqueous CF_3SO_3H vs SSCE

	$E_{1/2}$, V			
Ru(II) complex	Ru^{III}/Ru^{II}	Ru^{IV}/Ru^{III}	Ru^{V}/Ru^{IV}	Ru^{VI}/Ru^{V}
cis-$[(bpy)_2Ru(OH_2)_2]^{2+}$	0.65	~0.90[a]	1.10	1.26
cis-$[(4,4'\text{-dmbp})_2Ru(OH_2)_2]^{2+}$	0.52	~0.84	1.07	1.20
cis-$[(5,5'\text{-dmbp})_2Ru(OH_2)_2]^{2+}$	0.57	~0.86	1.08	1.20
cis-$[(6,6'\text{-dmbp})_2Ru(OH_2)_2]^{2+}$ [b]	0.72	0.87	1.10	1.45 (irr)

	$E_{1/2}$, V		
Ru(II) complex	Ru^{III}/Ru^{II}	Ru^{IV}/Ru^{III}	Ru^{VI}/Ru^{IV}
trans-$[(bpy)_2Ru(OH_2)_2]^{2+}$	0.44	0.88	1.01

[a] The Ru(IV)/Ru(III) couples are kinetically slow at the electrode. The waves typically have ΔE_p > 150 mV, and the $E_{1/2}$ values are only estimates. [b] From ref 2b.

The evidence obtained for oxidation states II → VI in the cyclic voltammetric studies is substantiated by the results of a Ce(IV) potentiometric titration. In the experiment 2.91 mg of *cis*-$[(bpy)_2Ru(CO_3)]\cdot 2H_2O$ were dissolved in 5 mL of 0.1 M aqueous CF_3SO_3H and titrated with 0.01 M $(NH_4)_2Ce(NO_3)_6$ in 0.1 M aqueous CF_3SO_3H. From Figure 4, breaks for the Ru(III)/Ru(II), Ru(IV)/Ru(III), and Ru(V)/Ru(IV) couples are clearly observed at $E_{1/2}$ values predicted by cyclic voltammetry with the Ru(VI)/Ru(V) couple less clear. An equivalent weight of 497 g/equiv calculated from the data is within experimental error of the actual formula weight of cis-$[(bpy)_2Ru(CO_3)]\cdot 2H_2O$ (M_r = 510).

Related Systems. As an extension of the earlier results obtained by Takeuchi et al.[3] and Che et al.,[5] pH dependences of the redox couples for the *trans*-diaqua isomer were also investigated. Representative cyclic voltammograms at pH 1.05 and 9.35 are shown in Figure 1b. The $E_{1/2}$–pH diagram resulting from the study is presented in Figure 3b. Additional data were acquired for the bpy-modified cis complexes, *cis*-$[(bpy')_2Ru^{II}(OH_2)_2]^{2+}$, where bpy' was the cis-diaqua analogue with either 4,4'-dimethyl-2,2'-bipyridine (4,4'-dmbp) or 5,5'-dimethyl-2,2'-bipyridine (5,5'-dmbp). Data for the various couples at pH 1 are presented

in Table I. The ^1H NMR spectra for *cis*-$[(bpy)_2Ru^{II}(OH_2)_2]^{2+}$ and *cis*-$[(5,5'\text{-dmbp})_2Ru^{II}(OH_2)_2]^{2+}$ are presented in Figure 5. The assignments of the cis bipyridine resonances were made by comparisons to the previously assigned spectrum for *cis*-$[(bpy)_2Ru^{II}(py)_2]^{2+}$.[14] Resonances for the methyl groups of the 5,5'-dmbp complex appear at 2.07 and 2.63 ppm.

Ligand Loss from Ru(VI). Addition of 4 equiv of Ce(IV) to an acidic solution containing *cis*-$[(bpy)_2Ru^{II}(OH_2)_2]^{2+}$ leads to a rapid color change. Upon the addition of Ce(IV), the intense MLCT bands in the visible region characteristic of Ru(II) disappear to give the essentially featureless spectrum of Ru(VI). Over an extended period (~60 min), a new band appears at 430 nm as shown in Figure 2b. The decomposition reaction led us to reinvestigate our controlled-potential electrolysis experiments. Bulk electrolysis of a solution containing 5×10^{-4} M *cis*-$[(bpy)_2Ru^{II}(OH_2)_2]^{2+}$ in 0.1 M aqueous CF_3SO_3H with E_{app} = 1.35 V vs SSCE occurred with $n = 3.8 \pm 0.2$, a value consistent with the generation of Ru(VI). However, cyclic voltammograms obtained before and after completion of the bulk electrolysis experiment (Figure 6) show that a change has occurred in chemical composition. After electrolysis a reversible wave appears at $E_{1/2}$ = 0.30 V and a quasi-reversible wave at $E_{1/2} \sim 0.92$ V ($\Delta E_p >$ 200 mV). Furthermore, waves characteristic of *cis*-$[(bpy)_2Ru^{II}(OH_2)_2]^{2+}$ derived redox couples are absent. Over a period of ~60 min the oxidized species is unstable as shown by the appearance of a band at 430 nm in the UV–vis spectrum. The appearance of the component absorbing at 430 nm does not follow simple first-order kinetics, and there was no further change in the cyclic voltammogram with time. The solution can be reoxidized at 1.35 V to its colorless form with the subsequent reappearance of the band at 430 nm after ~60 min. Addition of 2,2'-bipyridine to the reoxidized solutions increases the rate of growth of the 430-nm band. On an even longer time scale (12 h), the band at 430 nm decreases and a new band with a maximum at 646 nm appears, suggesting formation of a Ru(III)–Ru(III) μ-oxo ion.[2a,15] Nijs and co-workers[4] had previously observed bands at 430 and ~650 nm and assigned the band at 650 nm to formation of a μ-oxo ion but were unable to assign the band at 430 nm.

The overall sequence of reactions suggested by our observations is depicted in Scheme II. The results of a series of spectroelectrochemical experiments are consistent with Scheme II. A solution of **1** generated electrochemically and immediately reduced at 0.0 V to avoid formation of **2** gives the characteristic MLCT UV–vis spectrum of a Ru(II)–bpy complex, but as shown in Figure 6b, the spectrum is different in detail from the spectrum of *cis*-$[(bpy)_2Ru^{II}(OH_2)_2]^{2+}$. The loss in intensity and decrease in energy for the MLCT band are both consistent with loss of one of the two moderately back-bonding, chromophoric bpy ligands and replacement by water molecules in the inner coordination sphere. An identical experiment carried out in D_2O/0.1 M D_2SO_4 with ^1H NMR monitoring shows resonances centered at 8.89, 8.49, and 7.98 ppm (integration 1:2:1) vs DSS assignable to the free 2,2'-bipyridine ligand as determined by addition of free ligand to the solution. If a solution of **1** is reduced at E_{app} = 0.6 V, a spectrum with λ_{max} = 430 nm is obtained, once again, followed by slow formation of **3** with $\lambda_{max} \sim 646$ nm. From the spectral and electrochemical studies, we conclude that the Ru(VI) intermediate **1** is a mono(bipyridine) complex, that **2** is its Ru(III) analogue, and that the final reduction product is $[(bpy)Ru^{II}(OH_2)_4]^{2+}$. Consistent with the assignment of **2** as Ru(III) is the appearance of a shoulder at 312 nm, which originates in a $\pi \rightarrow \pi^*$ bpy-localized transition and is a useful marker for Ru(III) in *cis*- and *trans*-$[(bpy)_2Ru^{III}(OH_2)_2]^{3+}$, $[(bpy)_2Ru^{III}(OH_2)(OH)]^{2+}$, *cis*-$[(bpy)_2(py)Ru^{III}(OH_2)]^{3+}$, and *cis*-$[(bpy)_2(py)Ru^{III}(OH)]^{2+}$.[7b,12]

Attempts to isolate *cis*-$[(bpy)_2Ru^{VI}(O)_2](ClO_4)_2$ by addition of 4 equiv of Ce(IV) to acidic (1 M aqueous $HClO_4$) solutions containing *cis*-$[(bpy)_2Ru^{II}(OH_2)_2]^{2+}$ led to the formation of a pale yellow powder, which rapidly decomposed to a brown solid. In a previous communication the IR spectrum of the isolated solid was reported,[3] but in retrospect, the material isolated was almost surely impure and contaminated with the bpy loss product. Controlled-potential electrolysis of *cis*-$[(bpy)_2Ru^{II}(OH_2)_2]^{2+}$ at E_{app} = 1.15 V (pH 1) gives *cis*-$[(bpy)_2Ru^{V}(O)(OH)]^{2+}$, which is stable with respect to ligand loss as shown by cyclic voltammetry. However, at least in acidic solution, slow ligand loss does occur by a pathway believed to involve initial disproportionation to give *cis*-$[(bpy)_2Ru^{IV}(O)(OH_2)]^{2+}$ and *cis*-$[(bpy)_2Ru^{VI}(O)_2]^{2+}$ followed by bpy loss from Ru(VI).

In contrast to the *cis*-dioxo complex, *trans*-$[(bpy)_2Ru^{VI}(O)_2]^{2+}$ in acidic solution is stable with respect to ligand loss for extended periods (>1 h) as evidenced by the failure of new redox couples associated with the ligand loss complex to appear in the cyclic voltammogram.

Oxidation of H_2O. In a typical experiment, 5 mg (9.8×10^{-6} mol) of *cis*-$[(bpy)_2Ru(CO_3)]\cdot 2H_2O$ dissolved in 2 mL of 0.1 M aqueous CF_3SO_3H and 270 mg (~50 equiv) of $(NH_4)_2Ce(NO_3)_6$ dissolved in 1 mL of 0.1 M aqueous CF_3SO_3H were placed in separate compartments of an airtight two-compartment cell. The solutions were degassed with N_2 for 45 min after which time the gas above the solutions was analyzed by GC to ensure the absence of O_2 prior to mixing. After mixing, visible bubbles could be observed, and the gas above the reaction mixture was sampled for GC analysis. Yields of up to $\sim 1.5 \times 10^{-5}$ mol of O_2 were obtained. However, the reaction mixture did not remain homogeneous, and deposits of RuO_2 were detected. There was no evidence in the solution for the known water oxidation catalyst $[(bpy)_2(OH_2)Ru(O)Ru(OH_2)(bpy)_2]^{4+}$ (λ_{max} = 640 nm). Our results are consistent with those of Collin and Sauvage[2b] in suggesting that *cis*-$[(bpy)_2Ru^{VI}(O)_2]^{2+}$ is not an active catalytic component for the oxidation of water, a role that in this system may be played by RuO_2.

Scheme II. 5×10^{-4} M *cis*-$[(bpy)_2Ru^{II}(OH_2)_2]^{2+}$ in 0.1 M Aqueous CF_5SO_3H, pH 1

$$cis\text{-}[(bpy)_2Ru^{II}(OH_2)_2]^{2+} \underset{+4e^-,\,+4H^+}{\overset{4e^-,\,-4H^+}{\rightleftharpoons}} cis\text{-}[(bpy)_2Ru^{VI}(O)_2]^{2+}$$

$$cis\text{-}[(bpy)_2Ru^{VI}(O)_2]^{2+} \xrightarrow{\text{seconds}} \mathbf{1}\ (Ru^{VI},\ \text{no visible absorption})$$

$$\mathbf{1} \xrightarrow{\text{minutes}} \mathbf{2}\ (Ru^{III},\ \lambda_{max,vis}\ \text{at 430 nm})$$

$$\mathbf{2} \xrightarrow{>12\ h} \mathbf{3}\ (Ru^{III}\text{–O–}Ru^{III},\ \lambda_{max,vis}\ \text{at 646 nm})$$

Discussion

***cis*- and *trans*-$[(bpy)_2Ru^{II}(OH_2)_2]^{2+}$.** Earlier work has shown that the accessibility of hydroxo/oxo forms of the higher oxidation states of Ru and Os from the corresponding aqua complexes results in the availability of oxidation states II → VI over a remarkably narrow redox potential range.[3,5,16] From the $E_{1/2}$ vs pH plot for *cis*-$[(bpy)_2Ru^{II}(OH_2)_2]^{2+}$ in Figure 3a, oxidation states II → VI are accessible over a potential range of only ~0.6 V. In the pH domain 1.7–4.5 the potentials of the couples change ~59 mV/pH unit as predicted by the Nernst equation for couples involving loss of both one H^+ and one electron. The data are consistent with the sequential series of redox steps (b is 2,2'-bipyridine).

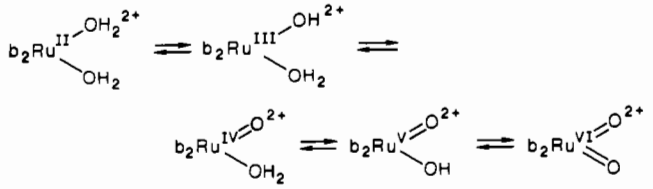

(14) Constable, E. C.; Seddon, K. R. *J. Chem. Soc., Chem. Commun.* **1982**, 34.

(15) Weaver, T. R.; Meyer, T. J.; Adeyemi, S. A.; Brown, G. M.; Eckberg, R. P.; Hatfield, W. E.; Johnson, E. C.; Murray, R. W.; Untereker, D. *J. Am. Chem. Soc.* **1975**, *97*, 3039.

(16) (a) Takeuchi, K. J.; Thompson, M. S.; Pipes, D. W.; Meyer, T. J. *Inorg. Chem.* **1984**, *23*, 1845. (b) Pipes, D. W.; Meyer, T. J. *Inorg. Chem.* **1986**, *25*, 4042. (c) Dobson, J. C.; Takeuchi, K. J.; Pipes, D. W.; Geselowitz, D. A.; Meyer, T. J. *Inorg. Chem.* **1986**, *25*, 2357.

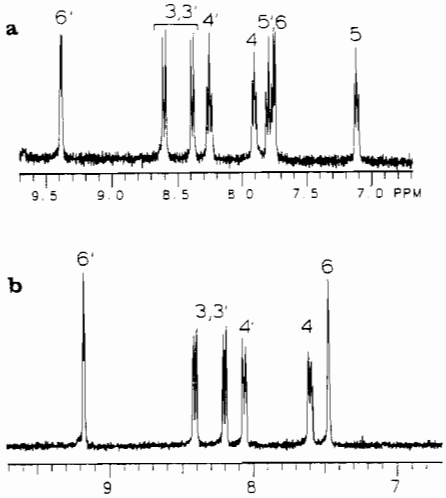

Figure 5. ^{1}H NMR spectra of (a) *cis*-$[(bpy)_2Ru^{II}(OH_2)_2]^{2+}$ and (b) *cis*-$[(5,5'\text{-dmbp})_2Ru^{II}(OH_2)]^{2+}$ in D_2O referenced vs DSS. The primed notation refers to those two of the four pyridyl rings of the bipyridyl ligands that are trans to one another.[14]

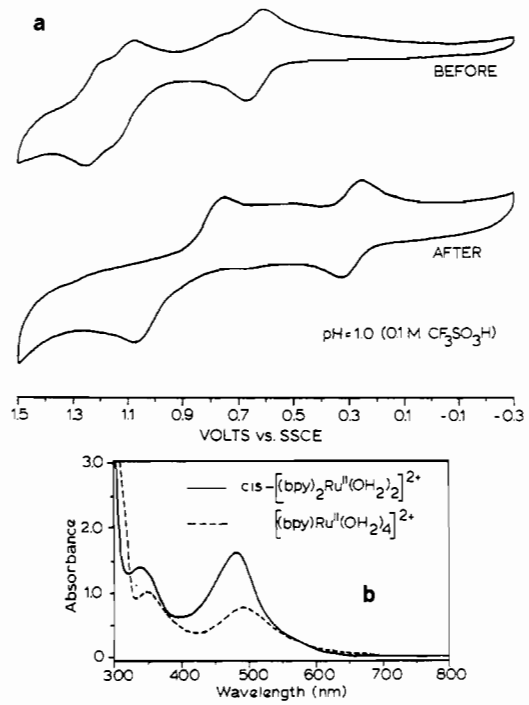

Figure 6. (a) Cyclic voltammograms obtained before and after controlled-potential electrolysis at 1.35 V vs SSCE of a solution containing *cis*-$[(bpy)_2Ru^{II}(OH_2)_2]^{2+}$ in 0.1 M aqueous CF_3SO_3H. (b) UV–vis spectra of *cis*-$[(bpy)_2Ru^{II}(OH_2)_2]^{2+}$ (2.0×10^{-4} M) in 0.1 M aqueous CF_3SO_3H (—) and the same solution obtained after controlled-potential electrolysis at 1.35 V vs SSCE immediately followed by controlled-potential electrolysis at 0.00 V vs SSCE (--).

This redox behavior is maintained up to pH ~4.5 where the pK_a for *cis*-$[(bpy)_2Ru^{V}(O)(OH)]^{2+}$ is reached, and at higher pH values the Ru(VI)/Ru(V) couple becomes pH-independent.

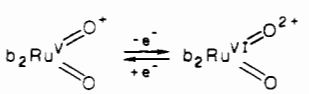

Experimental complications do exist for the cis couples arising from the slow electron-transfer chemistry associated with the Ru(IV)/Ru(III) couple and by apparent self-oxidation of the bpy ligand in basic solution. While no attempt was made to characterize the decomposition products in basic solution, new waves not associated with the *cis*-$[(bpy)_2Ru(OH_2)_2]^{2+}$-based redox couples appear in the cyclic voltammograms following oxidative sweeps past the $E_{1/2}$ values for the higher oxidation state couples

Table II. pK_a Values at μ = 0.1 M and 23 ± 2°

oxidn state	complex	M = Ru pK_{a1}	M = Ru pK_{a2}	M = Ru ref	M = Os pK_{a1}	M = Os pK_{a2}	M = Os ref
II	$[(NH_3)_5M^{II}(OH_2)]^{2+}$	13.1		19	12		20
	$[(trpy)(bpy)M^{II}(OH_2)]^{2+}$	9.7		16a	7.8		16a
	trans-$[(bpy)_2M^{II}(OH_2)_2]^{2+}$	9.2	>11.5	18	8.2	10.2	16c
	cis-$[(bpy)_2M^{II}(OH_2)_2]^{2+}$	8.9	>11	18	7.9	11	16c
III	$[(NH_3)_5M^{III}(OH_2)]^{3+}$	4.1		19	5.2		20
	$[(trpy)(bpy)M^{III}(OH_2)]^{3+}$	1.7		16a	2.0		16a
	trans-$[(bpy)_2M^{III}(OH_2)_2]^{3+}$	<1	~5.2	*c*	0.8	4.3	16c
	cis-$[(bpy)_2M^{III}(OH_2)_2]^{3+}$	~1.5	~5.2	*c*	~2.0	~5	16c
IV[a]	trans-$[(bpy)_2M^{IV}(O)(OH_2)]^{3+}$	~6–7		*c*	*b*		
	cis-$[(bpy)_2M^{IV}(O)(OH_2)]^{3+}$	~4–5		*c*	*b*		
V	cis-$[(bpy)_2M^{V}(O)(OH)]^{2+}$	~4.5		*c*	~5.8		16c

[a] These complexes are assumed to exist as the oxo–aqua forms rather than as the compositionally equivalent dihydroxo complexes. [b] Not available because of the instability of Os(IV) with respect to disproportionation. [c] This work.

in basic solution. Similar behavior has previously been documented in detail for $[Ru(bpy)_3]^{2+}$ [17a] and $[(bpy)_2(py)Ru^{II}(OH_2)]^{2+}$.[17b]

Approximate pK_a values can be estimated from the breaks in the slopes of the $E_{1/2}$–pH plots, and values obtained in our study are presented in Table II for the various oxidation states and compared with values obtained earlier for related complexes. The first pK_a value for *cis*-$[(bpy)_2Ru^{II}(OH_2)_2]^{2+}$ has been reported by Walsh et al. to be 8.9 as determined by a spectrophotometric titration,[18] which is in good agreement with the value estimated here electrochemically. The electrochemical irreversibility of the Ru(IV)/Ru(III) couple prevents an accurate determination of pK_{a1} for *cis*-$[(bpy)_2Ru^{IV}(O)(OH_2)]^{2+}$, and only an estimate of between 4 and 5 can be made.

From the data presented in the $E_{1/2}$–pH diagram for the trans complex in Figure 3b, which are consistent with the earlier observations of Che et al.,[5] evidence is also found for oxidation states II → VI although Ru(V) only appears as a stable oxidation state in basic solution. The potentials for the trans Ru(III)/Ru(II) and Ru(IV)/Ru(III) couples are decreased by ~210 mV compared to their cis analogues, but the most distinct feature in a comparative sense is the instability of oxidation state V in acidic solution. From pH 1 to 5 the decrease in $E_{1/2}$ values of 59 mV/pH unit is consistent with sequential $1e^-/1H^+$, $1e^-/1H^+$, and $2e^-/2H^+$ couples and the following scheme (bpy is N⁀N):

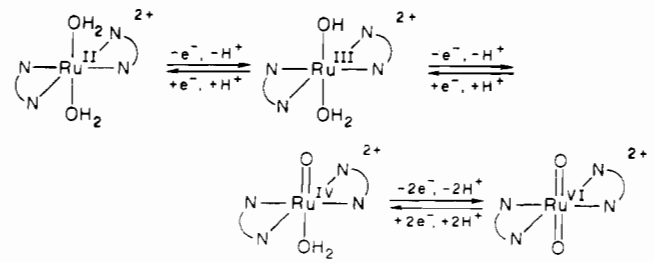

As a stable oxidation state Ru(V) appears only in basic solution.

(17) (a) Ghosh, P. K.; Brunschwig, B. S.; Chou, M.; Sutin, N. *J. Am. Chem. Soc.* **1984**, *106*, 4772. (b) Roecker, L.; Kutner, W.; Gilbert, J. A.; Simmons, M.; Murray, R. W.; Meyer, T. J. *Inorg. Chem.* **1985**, *24*, 3784. (c) Nord, G.; Pedersen, B.; Bjergbakke, E. *J. Am. Chem. Soc.* **1983**, *105*, 1913.
(18) Allen, L. R.; Craft, P. P.; Durham, B.; Walsh, J. *Inorg. Chem.* **1987**, *26*, 53.
(19) Kuehn, C.; Taube, H. *J. Am. Chem. Soc.* **1976**, *98*, 1976.
(20) (a) Gulens, J.; Page, J. A. *J. Electroanal. Chem. Interfacial Electrochem.* **1976**, *67*, 215. (b) Gulens, J.; Page, J. A. *J. Electroanal. Chem. Interfacial Electrochem.* **1974**, *55*, 239.

Table III. Reduction Potentials for Couples Involving the Cis and Trans Isomers of $[(bpy)_2M(OH_2)]^{2+}$ at pH 4.0 and 23 ± 2 °C in H_2O (μ = 0.1 M) vs SSCE[a]

	$E^{\circ\prime}$, V		$E^{\circ\prime}$,[b] V
	Cis Couples		
$b_2Ru^{VI}O)_2^{2+}/b_2Ru^{V}(O)(OH)^{2+}$	1.07	$b_2Os^{VI}(O)_2^{2+}/b_2Os^{V}(O)_2^{+}$	0.67
$b_2Ru^{V}(O)(OH)^{2+}/b_2Ru^{IV}(OH_2)^{2+}$	0.94	$b_2Os^{V}(O)(OH)^{2+}/b_2Os^{IV}(O)(OH_2)^{2+}$	0.48
$b_2Ru^{IV}(O)(OH_2)^{2+}/b_2Ru^{III}(OH)(OH_2)^{2+}$	0.76	$b_2Os^{IV}(O)(OH_2)^{2+}/b_2Os^{III}(OH_2)(OH)^{2+}$	0.41
$b_2Ru^{III}(OH)(OH_2)^{2+}/b_2Ru^{II}(OH_2)_2^{2+}$	0.50	$b_2Os^{III}(OH)(OH_2)^{2+}/b_2Os^{II}(OH_2)_2^{2+}$	0.04
	Trans Couples		
$b_2Ru^{VI}(O)_2^{2+}/b_2Ru^{IV}(O)(OH_2)^{2+}$	0.86	$b_2Os^{VI}(O)_2^{2+}/b_2Os^{III}(OH)(OH_2)^{2+}$	0.36
$b_2Ru^{IV}(O)(OH_2)^{2+}/b_2Ru^{III}(OH)(OH_2)^{2+}$	0.67		
$b_2Ru^{III}(OH)(OH_2)^{2+}/b_2Ru^{II}(OH_2)_2^{2+}$	0.30	$b_2Os^{III}(OH)(OH_2)^{2+}/b_2Os^{II}(OH_2)_2^{2+}$	−0.21

[a] b = bpy is 2,2′-bipyridine. [b] From ref 16c.

Past pH 8 the two-electron Ru(VI)/Ru(IV) couples splits into the pH-independent Ru(VI)/Ru(V) couple and the pH-dependent Ru(V)/Ru(IV) couple.

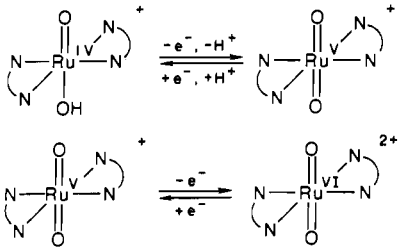

The thermodynamic instability of Ru(V) arises from the differences in the pH dependences of the Ru(VI)/Ru(V) and Ru(V)/Ru(IV) couples. Below pH 8, Ru(IV) becomes a stronger oxidizing agent than Ru(V) and Ru(V) is unstable with respect to disproportionation.

$$2[(bpy)_2Ru^{V}(O)_2]^{+} + H^{+} \rightarrow [(bpy)_2Ru^{IV}(O)(OH)]^{+} + [(bpy)_2Ru^{VI}(O)_2]^{2+}$$

The pK_a values for the various oxidation states estimated from the breaks in the $E_{1/2}$–pH plots in Figure 3 are listed in Table II. The value of pK_a = 9.2 for *trans*-$[(bpy)_2Ru^{II}(OH_2)_2]^{2+}$ is in good agreement with the value of 9.3 determined earlier by spectrophotometry.[18] From the plots, a pK_a value of ~6 can be approximated for *trans*-$[(bpy)_2Ru^{IV}(O)(OH_2)]^{2+}$. Over the pH range within which they are observable, both Ru(VI) and Ru(V) exist only as the deprotonated dioxo ions.

Comparisons between Structurally Equivalent Complexes of Ru and Os. The redox potential data acquired here and earlier for closely related polypyridyl complexes of Ru and Os provide a basis for discussing some fundamental issues that arise in the redox chemistry of transition-metal complexes in aqueous solution. The effects on the magnitudes of redox potentials of proton loss and hydroxo and oxo formation in higher oxidation states have been discussed.[16] An earlier comparison between related complexes of Re and Os was illustrative in revealing the effects of electronic structure.[21] With the Ru data in hand, a detailed comparison can now be made between electronically analogous complexes of second- and third-row congeners. The comparisons involve structurally equivalent complexes, and such factors as solvation energy differences should remain nearly constant. Variations in $E^{\circ\prime}$ values are largely dictated by intrinsic differences in the electronic and bonding properties of the two metals.

The redox potential data at pH 4.0 in Table III and the plot of those data vs redox couple for the cis couples in Figure 7 are of direct relevance in such comparisons. The data at pH 4.0 were chosen since at that pH each of the cis couples involves a singlet H^+ change, e.g.

$$cis\text{-}[(bpy)_2Ru^{III}(OH)(OH_2)]^{2+} + e^{-} + H^{+} \rightarrow cis\text{-}[(bpy)_2Ru^{II}(OH_2)_2]^{2+}$$

The effects on the potentials of proton loss are a constant feature

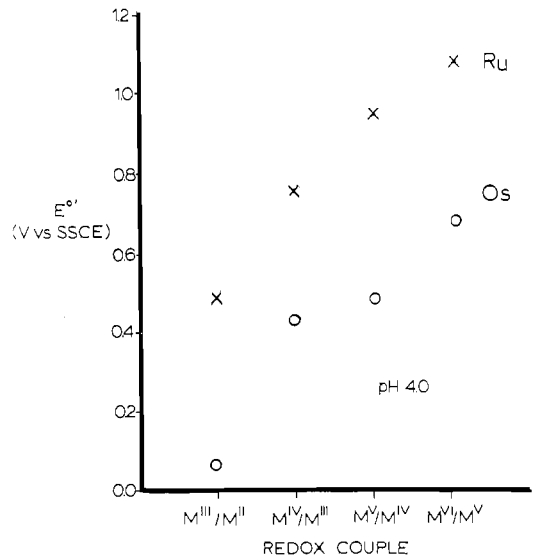

Figure 7. Plot of $E^{\circ\prime}$ values (vs SSCE) with oxidation state for couples derived from *cis*-$[(bpy)_2M(OH_2)_2]^{2+}$ (M = Ru, Os) at 25 °C in H_2O at pH 4.0 (μ = 0.1 M).

throughout the series. From the data several conclusions can be drawn:

1. As expected, for the cis couples in Figure 7 there is a steady increase in $E^{\circ\prime}$ as the oxidation states involved in the couples increase. The difference between successive couples actually *decreases* for the higher oxidation state couples pointing, once again, to the importance of electronic stabilization of the higher oxidation states by metal–oxo formation. The stabilization of the higher oxidation states of Ru and Os by oxo formation is sufficient that a series of oxidation states appear even within the somewhat restricted redox potential limits of water as the solvent. The couples involved span the range of d-electronic configurations from d^2/d^3 for the $[(bpy)_2M^{VI}(O)_2]^{2+}/[(bpy)_2M(O)(OH)]^{2+}$ couples to d^5/d^6 for the $[(bpy)_2M^{III}(OH)(OH)]^{2+}/[(bpy)_2M^{II}(OH_2)_2]^{2+}$ couples. However, with the exception of Os(IV), there is a monotonic increase in $E^{\circ\prime}$ with oxidation state. Rather than from specific electronic effects, the increase in potentials with oxidation state appears to arise from a general increase in electronic deficiency at the metal center.

2. The major differences between Ru and Os in both the cis and trans series occur at the M(III)/M(II) couples. $\Delta E^{\circ\prime} = E^{\circ\prime}_{Ru} - E^{\circ\prime}_{Os}$ is in the range 0.46–0.53 V for these couples. Decreases in potentials for the Os(III)/Os(II) couples for coordinatively equivalent complexes of Os and Ru are commonly observed.[16a,22] On the basis of an appropriate thermodynamic analysis, a major factor in the difference is the decrease in the third ionization energy for Os.[22] Additional contributions to the $E^{\circ\prime}$ values for the M(III)/M(II) couples are expected to exist from $d\pi \rightarrow \pi^*$(bpy) back-bonding in oxidation state M(II) and from σ- and π-donation

(21) Pipes, D. W.; Meyer, T. J. *Inorg. Chem.* **1986**, *25*, 3256.

(22) Buckingham, D. A.; Sargeson, A. M. In *Chelating Agents and Metal Chelates*; Dwyer, F. P., Mellor, D. P., Eds.; Academic: New York, 1964.

in oxidation state M(III). $d\pi \rightarrow \pi^*$(bpy) back-bonding is of more importance, as shown by the data in Table I. From the data, variations in redox potentials induced by changes in the bpy ligand occur largely at the Ru(III)/Ru(II) stage. Variations in the higher oxidation state couples, which should be dominated by σ- and/or π-electronic donation, are relatively small. The same trend appears when ligand variations are made at the fifth coordination site. At pH 4.0 the potentials for the Ru(IV)/Ru(III) couples *cis*-$[(bpy)_2(py)Ru(O)]^{2+}$/*cis*-$[(bpy)_2(py)Ru(OH)]^{2+}$ (0.71 V vs SSCE) and *cis*-$[(bpy)_2Ru(O)(OH_2)]^{2+}$/*cis*-$[(bpy)_2Ru(OH)(OH_2)]^{2+}$ (0.76 V vs SSCE) are comparable. However, replacement of the aqua group by the moderately back-bonding pyridyl group increases the potential of the Ru(III)/Ru(II) couple *cis*-$[(bpy)_2Ru(OH)(L)]^{2+}$/*cis*-$[(bpy)_2Ru(OH_2)(L)]^{2+}$ from 0.50 V for L = OH_2 to 0.60 V for L = py. The recognition of such ligand effects leads to the possibility of manipulating redox potentials systematically and helps to explain the domains of stability for individual oxidation states. For example, the substitution of py for OH_2 in the cis bipyridine series has the net effect of decreasing the potential difference between the Ru(IV)/Ru(III) and Ru(III)/Ru(II) couples to only ~110 mV, and over a broad pH range Ru(III) is only slightly unstable with respect to disproportionation.

$$2cis\text{-}[(bpy)_2(py)Ru^{III}(OH)]^{2+} \rightarrow cis\text{-}[(bpy)_2(py)Ru^{IV}(O)]^{2+} + cis\text{-}[(bpy)_2(py)Ru^{II}(OH_2)]^{2+}$$

In fact, in basic solution, past pK_{a1} for *cis*-$[(bpy)_2(py)Ru^{II}(OH_2)]^{2+}$, the Ru(III)/Ru(II) couple becomes pH-independent, *cis*-$[(bpy)_2(py)Ru^{III}(OH)]^{2+}$/*cis*-$[(bpy)_2(py)Ru^{II}(OH)]^{+}$, and Ru(III) becomes unstable with respect to disproportionation via

$$2[(bpy)_2(py)Ru^{III}(OH)]^{2+} + OH^- \rightarrow [(bpy)_2(py)Ru^{II}(OH)]^{+} + [(bpy)_2(py)Ru^{IV}(O)]^{2+} + H_2O$$

3. The odd man out in the monotonic increases in $E^{\circ\prime}$ with oxidation state in Figure 7 is Os(IV). The potential difference between the M(V)/M(IV) and M(IV)/M(III) couples is small (0.07 V) and that between the M(IV)/M(III) and M(III)/M(II) couples is large (0.37 V) for Os(IV) compared to Ru. The electronic origin of the implied instability of Os(IV) is unclear but a contributing factor could lie in a relatively high fourth ionization energy for Os. The fact that the destabilizing effect does exist has important consequences for the underlying redox chemistry. For the cis series of couples, the Os(IV)/Os(III) couple is so near to the potential of the Os(V)/Os(IV) couple that differences in proton content between the Os(V)/Os(IV) and Os(IV)/Os(III) couples lead to Os(IV) being thermodynamically unstable with respect to disproportionation into Os(V) and Os(III) over all but a narrow pH range (2–5) in water.[16c]

4. As observed earlier for the analogous Os couples,[16c] stereochemical effects, cis vs trans, play an important role in affecting $E^{\circ\prime}$ values. In the trans stereochemistry the M(III)/M(II) couples are less oxidizing than the cis couples by ~200–250 mV, implying a stabilization of Ru(III) and/or a destabilization of Ru(II) in the trans geometry. In the trans complexes significant steric interactions exist between the 6 and 6′ protons of the bpy ligands, leading to noticeable distortion from coplanarity.[7b,d] However, the most important electronic effect may come from a significant loss in $d\pi \rightarrow \pi^*$(bpy) back-bonding for the trans isomer in oxidation state II. That such effects play an important role for the Ru(III)/Ru(II) couple is shown by the fact that potentials for both the cis and trans Ru(V)/Ru(IV) couples, where metal to ligand back-bonding is unimportant, are within 30 mV of each other.

5. Of equal importance, but in the opposite direction, is the effect of electronic stabilization of the *trans*-dioxo $(d\pi)^2$ structure in *trans*-$[(bpy)_2M(O)_2]^{2+}$ relative to the cis isomer.[16c] Electronic stabilization at the M(VI) *trans*-dioxo stage is sufficient to decrease the potential of the Ru(VI)/Ru(V) $[(bpy)_2Ru(O)_2]^{2+/+}$ couple from ~1.04 V for the cis couple to 0.73 V for the trans couple (pH 9.0, Figure 3). In solutions more acidic than pH ~7, $E^{\circ\prime}$ for the Ru(VI)/Ru(V) couple falls below $E^{\circ\prime}$ for the Ru(V)/Ru(IV) couple. Below this pH, Ru(V) is a stronger oxidizing agent than is Ru(VI) because of the different pH dependences of the couples, and Ru(V) is unstable with respect to disproportionation:

$$2trans\text{-}[(bpy)_2Ru^{V}(O)_2]^{+} + 2H^+ \rightarrow trans\text{-}[(bpy)_2Ru^{VI}(O)_2]^{2+} + trans\text{-}[(bpy)_2Ru^{IV}(O)(OH_2)]^{2+}$$

or

$$2trans\text{-}[(bpy)_2Ru^{V}(O)(OH)]^{2+} \rightarrow trans\text{-}[(bpy)_2Ru^{VI}(O)_2]^{2+} + trans\text{-}[(bpy)_2Ru^{IV}(O)(OH_2)]^{2+}$$

The relative instability of Os(IV) creates an even more dramatic situation for the equivalent trans couples of Os. For the trans series of couples, the instability of Os(IV) increases the Os(IV)/Os(III) couple above the Os(V)/Os(IV) couple and Os(IV) is unstable with respect to disproportionation. That fact combined with the stabilization of *trans*-$[(bpy)_2Os(O)_2]^{2+}$ leads to the appearance of only the Os(VI)/Os(III) couple *trans*-$[(bpy)_2Os(O)_2]^{2+}$/*trans*-$[(bpy)_2Os(OH)(OH_2)]^{2+}$ in acidic solution.

A comparative summary of acid dissociation constants for a series of aqua and hydroxo complexes of Ru and Os obtained by either electrochemical or titration measurements is given in Table II. From the data it can be seen that for structurally analogous polypyridyl aqua complexes of Ru(II) and Os(II), the Os(II) complexes are slightly more acidic. The origin of the enhanced acidity may be in a greater degree of Os–OH_2 mixing in the Os(II)–OH_2 bond due in part to greater $d\pi$(Os) $\rightarrow \pi^*$(bpy) back-bonding for Os(II).[23] Oxidation to M(III) leads to a remarkable enhancement in acidity, the enhancement being a factor of ~10^8 in K_{a1} for *cis*-$[(bpy)_2Ru^{III}(OH_2)_2]^{3+}$. The impact of metal–oxo formation appears in the pK_a value for Ru(IV). Metal–oxo formation leaves the metal between oxidation states II and III in terms of the acidity of the bound water molecule.

Ligand Loss and Reduction of Ru(VI). In aqueous solution *cis*-$[(bpy)_2Os^{VI}(O)_2]^{2+}$ is unstable with respect to loss of bpy via the net reaction

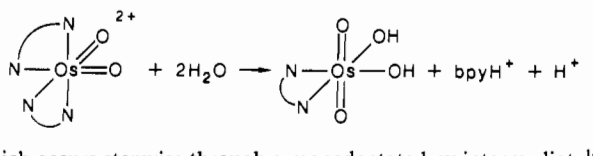

which occurs stepwise through a monodentate bpy intermediate[16c]

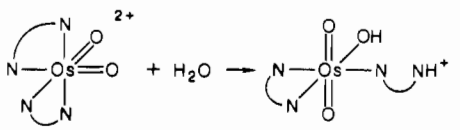

The driving force for bpy loss and rearrangement is the electronic stabilization arising from the *trans*-dioxo arrangement at d^2 Os(VI), and the appearance of chelate ring opening suggests that a facile trans → cis intramolecular rearrangement pathway does not exist.

The coordination chemistry of Ru(VI) appears to be analogous in that, following oxidation to Ru(VI)

$$cis\text{-}[(bpy)_2Ru^{II}(OH_2)_2]^{2+} \underset{+4e^-,\,+4H^+}{\overset{-4e^-,\,-4H^+}{\rightleftharpoons}} cis\text{-}[(bpy)_2Ru^{VI}(O)_2]^{2+}$$

bpy ligand loss also occurs.

$$cis\text{-}[(bpy)_2Ru^{VI}(O)_2]^{2+} \rightarrow trans,cis\text{-}(bpy)Ru^{VI}(O)_2(OH)_2 + bpy$$

However, for Ru the chemistry is further complicated by subsequent reduction of Ru(VI), at least in part, by reduction by bpy freed in the ligand loss step.

$$bpy + trans,cis\text{-}(bpy)Ru^{VI}(O)_2(OH)_2 \rightarrow [(bpy)Ru^{III}(OH_2)_3(OH)]^{2+} + bpy_{ox}$$

The proton contents of the bpy-loss Ru(III) and Ru(VI) complexes

(23) Taube, H. *Pure Appl. Chem.* **1979**, *51*, 901.

are only surmised and will depend on pH. For example, the first proton loss from *cis*-$[(bpy)_2Ru^{III}(OH_2)_2]^{3+}$ occurs with $pK_a \sim 1.5$ (25 °C, μ = 0.1 M, Table II). The bpy-loss Ru(III) complex is probably comparably acidic. The complex *trans,cis*-$(bpy)Os^{VI}(O)_2(OH)_2$ has been isolated from acidic solution.[16c]

No attempt was made to characterize the product of the bpy oxidation. Earlier work has shown that oxidation of *coordinated* bpy in $[Ru^{III}(bpy)_3]^{3+}$, $[(bpy)_2(py)Ru^{IV}(O)]^{2+}$ (py is pyridine), or $[Fe(bpy)_3]^{3+}$ does occur at reasonable rates in basic solution[17,24] and that the net chemistry involves ring oxidation and/or *N*-oxide formation. Ring oxidation could be occurring here or, more likely, oxidation to give the *N*-oxide.

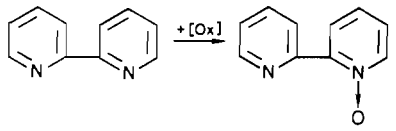

While the *cis*-dioxo stereochemistry of the M(VI) leads to ligand loss on the time scale of seconds as shown by ^1H NMR (Results), the *trans*-dioxo complexes *trans*-$[(bpy)_2Ru^{VI}(O)_2]^{2+}$ and *trans*-$[(bpy)_2Os^{VI}(O)_2]^{2+}$ are stable with respect to ligand loss in acidic solution for extended periods (>1 h) as evidenced by the lack of observed changes in the cyclic voltammograms.

Electrochemical and spectral studies show that in acidic aqueous solution the d^3 Ru(V) ion *cis*-$[(bpy)_2Ru(O)(OH)]^{2+}$ is coordinatively stable. For Ru(V) the special electronic stabilization associated with the d^2 *trans*-dioxo structure is lost, and the result is expected. However, a pathway for slow ligand loss does exist in solution that appears to involve initial disproprtionation

$$2[(bpy)_2Ru^{V}(O)(OH)]^{2+} \rightarrow [(bpy)_2Ru^{VI}(O)_2]^{2+} + [(bpy)_2Ru^{IV}(O)(OH_2)]^{2+}$$

followed by ligand loss from Ru(VI). From the $E_{1/2}$–pH diagram in Figure 3a, the initial disproportionation step is nonspontaneous at all pH values ($E^{\circ\prime} \sim 110$ mV from pH 1 to 5) and becomes increasingly less favorable as the pH is increased past pH 5, where the net reaction is

$$2[(bpy)_2Ru^{V}(O)(OH)]^{2+} \rightarrow [(bpy)_2Ru^{VI}(O)_2]^{2+} + [(bpy)_2Ru^{IV}(O)(OH)]^{+} + H^+$$

Needless to say, the appearance of the ligand loss chemistry at oxidation state M(VI) is a disappointing yet, in retrospect, predictable result. The trans complexes themselves are proving to be useful stoichiometric and/or catalytic oxidants. However, the ligand loss chemistry is frustrating given the greater thermodynamic oxidizing strength of the *cis*- compared to the *trans*-dioxo couples and the mechanistic advantages implied by the *cis*-dioxo structure with regard to mimicking the reactivity of RuO_4 or OsO_4 and exploiting that reactivity catalytically. If the implied advantages of the M(VI) *cis*-dioxo structure are to be exploited, it seems clear that careful attention must be paid to ligand design.

Implications. The redox potential data presented here bear on the emerging theme of the rational design of water oxidation catalysts. The oxidation of water involves a four-electron change with O–O coupling.

$$2H_2O \rightarrow O_2 + 4e^- + 4H^+$$

The demands on a single molecular site, if it is to act catalytically, include the existence of four-electron couples based on that site. By now, a number of four-electron couples based on polypyridyl complexes of Ru and Os have been identified and their reduction potentials as a function of pH from pH 0 to 7 are shown in Figure 8 compared to the O_2/H_2O couple. The data show that of all the couples studied only the four-electron couples based on the oxo-bridged Ru(V)–Ru(V) complex $[(bpy)_2(O)Ru^{V}ORu^{V}(O)(bpy)_2]^{4+}$ and *cis*-$[(bpy)_2Ru^{VI}(O)_2]^{2+}$ are thermodynamically capable of water oxidation. The μ-oxo Ru complex is a stoichiometric and catalytic reagent for the oxidation of water, and it has been proposed that the crucial redox step may involve a synchronous, intramolecular four-electron change from Ru(V)–Ru(V) to Ru(III)–Ru(III).[2a] In principle, *cis*-$[(bpy)_2Ru(O)_2]^{2+}$ has the same capability but at a single site

$$cis\text{-}[(bpy)_2Ru^{VI}(O)_2]^{2+} + 2H_2O \rightarrow cis\text{-}[(bpy)_2Ru^{II}(OH_2)_2]^{2+} + O_2$$

Although such a pathway may exist, it is hidden in the cis complex because of the instability of the complex with regard to loss of a bpy ligand.

Alternate pathways for water oxidation may also exist, but they necessarily involve more than one site, e.g.

$$2\,trans\text{-}[(bpy)_2Ru^{VI}(O)_2]^{2+} + 2H_2O \rightarrow 2\,trans\text{-}[(bpy)_2Ru^{IV}(O)(OH_2)]^{2+} + O_2$$

$$\Delta G^{\circ\prime} = -0.02 \text{ V, pH } 1$$

or high energy intermediates, e.g.,

$$cis\text{-}[(bpy)_2Ru^{VI}(O)_2]^{2+} + H_2O \rightarrow cis\text{-}[(bpy)_2Ru^{V}(O)(OH)]^{2+} + OH$$

$$\Delta G^{\circ\prime} = 0.72 \text{ V, pH } 1$$

with their attendant mechanistic complexities and disadvantages with regard to rate.

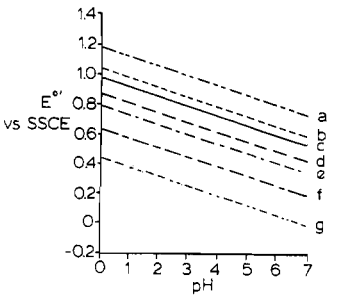

Figure 8. Variation in reduction potentials, in V vs SSCE, for a series of four-electron couples: (a) $[(bpy)_2(O)Ru^{V}ORu^{V}(O)(bpy)_2]^{4+}/[(bpy)_2(OH_2)Ru^{III}ORu^{III}(OH_2)(bpy)_2]^{4+}$; (b) *cis*-$[(bpy)_2Ru^{VI}(O)_2]^{2+}/cis\text{-}[(bpy)_2Ru^{II}(OH_2)_2]^{2+}$; (c) O_2/H_2O; (d) *trans*-$[(bpy)_2Ru^{VI}(O)_2]^{2+}/trans\text{-}[(bpy)_2Ru^{II}(OH_2)_2]^{2+}$; (e) $[(bpy)_2(O)Os^{V}OOs^{V}(O)(bpy)_2]^{4+}/[(bpy)_2(OH_2)Os^{III}OOs^{III}(OH_2)(bpy)_2]^{4+}$; (f) *cis*-$[(bpy)_2Os^{VI}(O)_2]^{2+}/cis\text{-}[(bpy)_2Os^{II}(OH_2)_2]^{2+}$; (g) *trans*-$[(bpy)_2Os^{VI}(O)_2]^{2+}/trans\text{-}[(bpy)_2Os^{II}(OH_2)_2]^{2+}$.

Acknowledgments are made to the National Science Foundation under Grant No. CHE-8601604 and to the National Institutes of Health under Grant No. 5-R01-GM32296-05 for support of this research. We also acknowledge D. Geselowitz for assistance in the potentiometric titration experiment and J. Gilbert for assistance with the pH-dependent electrochemical experiments.

Registry No. 4,4′-dmpb, 1134-35-6; 5,5′-dmpb, 1762-34-1; *cis*-$[(bpy)_2Ru(CO_3)]$, 59460-48-9; *trans*-$[(bpy)_2Ru^{II}(OH_2)_2](CF_3SO_3)_2$, 115890-20-5; *cis*-$[(5,5'\text{-dmpb})_2RuCl_2]$, 115890-21-6; *cis*-$[(4,4'\text{-dmpb})_2RuCl_2]$, 68510-55-4; *cis*-$[(4,4'\text{-dmpb})_2Ru(CO_3)]$, 115890-22-7; *cis*-$[(5,5'\text{-dmpb})_2Ru(CO_3)]$, 115890-23-8; H_2O, 7732-18-5; O_2, 7782-44-7.

(24) Creutz, C.; Sutin, N. *Proc. Natl. Acad. Sci. U.S.A.* **1975**, *72*, 2859.